SPECTRAL UNMIXING FOR THE CLASSIFICATION OF HYPERSPECTRAL IMAGES

Yi-Hsing TSENG
National Cheng Kung University, China-Taipei
Department of Surveying Engineering
Tseng@mail.ncku.edu.tw

Working Group VII/2

KEY WORDS: Spectral Unmixing, Hyperspectral, Sub-pixel Classification, Least Squares Unmixing, Matched Filter Unmixing, Maximum Noise Fraction Transformation, Remote Sensing.

ABSTRACT

Spectral mixing is inherent in any finite-resolution digital imagery of a heterogeneous surface, so that mixed pixels are inevitably created when multispectral images are scanned. Solving the spectral mixture problem is, therefore, involved in image classification, referring to the techniques of spectral unmixing. The invention of imaging spectrometers especially promotes the potential of applying spectral unmixing for sub-pixel classification. This paper investigates two spectral unmixing techniques: the least squares (LS) unmixing and the matched filter (MF) unmixing. Experiments with a set of AVIRIS data were carried out to evaluate the performance of spectral unmixing. The MF unmixing method proved itself to be an effective technique in classifying a hyperspectral image by showing a 90% classification accuracy. Whereas, the LS unmixing technique did not show promising results, when it was applied to the original bands of the test image. The maximum noise fraction (MNF) transformation, however, is found to be helpful to promote the performance of the LS unmixing. Applying the LS unmixing to the MNF transformed images can improve the classification accuracy for about 20%.

1 INTRODUCTION

In remote-sensing imagery, the measured spectral radiance of a pixel is the integration of the radiance reflected from all the objects within the ground instantaneous field of view (GIFOV). Mixed pixels are generated if the size of the pixel includes more than one type of terrain cover. Obviously, spectral mixing is inherent in any finite-resolution digital imagery of a heterogeneous surface. Solving the spectral mixture problem (Horwitz et al., 1971) is, therefore, involved in image classification, referring to the techniques of spectral unmixing. Spectral unmixing is developed based on the assumption that a pixel composed of multiple components, with known *a prior* knowledge of their pure signatures, can be mathematically approximated using a linear mixture model. Fraction coefficients, representing the proportions of components within a pixel, can be calculated after unmixing. Sub-pixel image classification is, therefore, possible to complete through the computation of spectral unmixing. Although the proposition of spectral unmixing can be dated to the earliest of Landsat, its applications in remote sensing were limited due to the low spectral resolution of the sensors in the past. The invention of imaging spectrometers (Goetz et al., 1985) promotes the application potential of spectral unmixing in terms of sub-pixel classification.

Imaging spectrometers measure spectral radiance with high spectral resolution and produce spectral data in tens or hundreds of bands, as called hyperspectral images. With the large number of bands, traditional supervised classification techniques become awkward, because the classification process needs to be done in high dimensional feature space. Spectral unmixing, however, does not rely on the statistic data of point distribution in the feature space, so that it is computationally simple and feasible to hyperspectral data processing. In addition, the large number of spectral bands in hyperspectral data aids spectral unmixing in two ways. First, it allows the unmixing of very complex scenes to avoid intrinsic singular problems. Second, the high spectral resolution of hyperspectral data permits the direct identification of image-derived endmember spectra (Boardman, 1994). To study the capability of spectral unmixing for the classification of hyperspectral images, this paper investigates two spectral unmixing techniques: the least squares (LS) unmixing and the matched filter (MF) unmixing. Experiments with a set of AVIRIS data were carried out to evaluate the performance of spectral unmixing. The maximum noise fraction (MNF) transformation is also tried to promote the performance of the LS unmixing.

Hyperspectral image bands are often highly correlated and among them some of absorption bands contain little signal but noise. Analysis of all of the original spectral bands not only is inefficient but also tends to create poor results. In

this paper, the maximum noise fraction (MNF) transformation (Green et al., 1988) is applied to segregate noises and to reduce the data dimensionality. This procedure promotes the performance of the LS unmixing.

2 SUB-PIXEL CLASSIFICATION

2.1 Linear Mixture Model

With known number of endmembers and giving the spectra of each pure component, the observed pixel value in any spectral band is modeled by the linear combination of the spectral response of component within the pixel. This linear mixture model can be mathematically described as a set of linear vector-matrix equation,

$$P_i = \sum_{j=1}^{n} (R_{ij} \cdot F_j) + E_i \qquad (1)$$

where:

$i = 1,\ldots,m$ (number of bands);
$j = 1,\ldots,n$ (number of endmembers);
P_i = spectral reflectance of the ith spectral band of a pixel;
R_{ij} = known spectral reflectance of the jth component;
F_j = the fraction coefficient of the jth component within the pixel;
E_i = error for the ith spectral band.

The error terms account for the unmodeled reflectance and represent the unknown noise of observations. Expanding (1) to all spectral bands gives the matrix form of the linear unmixing equations

$$P = RF + E \qquad (2)$$

where

$$P = \begin{bmatrix} P_1 \\ P_2 \\ \vdots \\ P_m \end{bmatrix}; \quad R = \begin{bmatrix} R_{11} & R_{12} & \ldots & R_{1n} \\ R_{21} & R_{22} & \ldots & R_{2n} \\ \vdots & \vdots & \vdots & \vdots \\ R_{m1} & R_{m2} & \ldots & R_{mn} \end{bmatrix}; \quad F = \begin{bmatrix} F_1 \\ F_2 \\ \vdots \\ F_n \end{bmatrix}; \quad E = \begin{bmatrix} E_1 \\ E_2 \\ \vdots \\ E_m \end{bmatrix}.$$

A physical realistic solution to the linear unmixing problem requires that 1) the sum of the coefficients equals one to ensure the whole pixel area is represented in the model and 2) each of the fraction coefficients be nonnegative to avoid negative subpixel areas. While the first requirement can be modeled by a constraint equation, for the second requirement, the coefficients need to be constrained by inequalities

$$\sum_{j=1}^{n} F_j = 1 \quad \text{and} \quad F_j \geq 0, \text{ for } j = 1,\ldots,n \qquad (3)$$

These constraints could be problematic, since one is never sure that a sufficient number of endmembers have been defined for a given set of data.

2.2 Least-Squares (LS) Linear Unmixing

The linear unmixing is an inversion problem of equation (2) with an observed vector P and a given matrix R to solve F. To obtain a unique solution for the inversion problem, it is assumed that the number of spectral bands m is greater than the number of endmembers n in the pixel. In the least-squares approach (Shimabukuro and Smith, 1991) to the inversion problem, the unmixing coefficients are found by minimizing the sum of the squares of the errors. When the constraints listed in equation (3) are ignored, it is equivalent to solving a set of equations of the form

$$\frac{\partial}{\partial F_j}\left[\sum_{i=1}^{m}\left(P_i - \sum_{j=1}^{n} R_{ij}F_j\right)^2\right] = 0 \qquad (4)$$

Expansion of (4) results in the classical multiple linear regression matrix equation, and the least-squares fit estimation on the unmixing coefficients F_j will be

$$\hat{F} = \left(R^T R\right)^{-1} R^T P \qquad (5)$$

Taking the difference of the observed and the calculated spectral reflectance results in the estimated error terms of the observations

$$\hat{E} = P - R\hat{F} \qquad (6)$$

The variance of the error terms is a quantitative measure of how the mixture modeling fits the data, which indicates the feasibility of the solution. The estimation of the variance is

$$\hat{\sigma}_E = \sqrt{E \cdot E/(m-n)} \qquad (7)$$

The least-squares solution can be modified to fulfill the requirements of constrained fits. For the first requirement, the estimated coefficients F_j are modified by taking the linear constraints $AF = b$ into account

$$\hat{F} = (R^T R + A^T A)^{-1}(R^T P + A^T b) \qquad (8)$$

Where A is an 1 by n matrix as follows:

$$A = [1 \quad 1 \quad \ldots \quad 1]; \qquad b = [1]$$

No analytical solutions are known for the inversion problem when the coefficients are constrained by inequalities. The use of iterative approaches like the simplex method is needed to implement those constraints (Pesses, 1999).

2.3 Matched Filter (MF) Unmixing

Based on well-known signal processing methodologies, the approach of matched filter unmixing maximizes the response of a known endmember and suppresses the response of the composite unknown background, thus matching the known signature. In this approach, a set of orthogonal matched filter vectors M are constructed to estimate the unmixing coefficients via a dot product with the observed pixel spectra as follows:

$$\hat{F} = M \cdot P \qquad (9)$$

Each filter vector is chosen to maximize the signal-to-noise ratio and is orthogonal to all endmember spectra except the one that it represents. Derived using the calculus of variations, Bowles et al. (1995) proposed a set filter vectors for the unmixing problem

$$M = (DR)^{-1} D \qquad (10)$$

where

$$D = R^T - \left(\frac{U}{m} R\right)^T$$

and U is an n by m matrix with each element = 1.

Matched filter provides a rapid means of detecting spectral similarities based on matches to specific endmember spectra. The results of filtering an image are usually presented as n gray-scale images with values from 0 to 1.0, which provide a means of estimating relative degree of match to the reference spectrum.

3 NOISE SEGREGATION AND DIMENSION REDUCTION

Hyperspectral image bands are often highly correlated and among them some of absorption bands contain little signal but noise. Analysis of all of the original spectral bands not only is inefficient but also tends to create poor results. The application of the LS unmixing is one of the examples, especially when it is applied to hyperspectral images. The LS unmixing is quite sensitive to image noise, because it is based on the assumption that the image has random noise and no correlation between wavebands. Therefore, noise segregation and dimension reduction are essential procedures need to be performed prior to applying the LS unmixing.

For extracting the most signal from a multispectral image, the principal component (PC) transformation is often applied to produce components that show decreasing image quality with increasing component number. However, due to the high between-band correlation, the transformation may lead to generate low-order principal components (Singh and Harrison, 1985). The maximum noise fraction (MNF) transformation is therefore proposed by Green et al. (1988) to produce components ordered by image quality. The MNF transform was derived as an analogue of the PC transform, where the criterion for the generation of the components is that they maximize the noise content represented by each component, rather than the data variance. In reverse order these components maximize the signal-to-noise ratio (SNR)

represented by each component. The MNF transform is a two-step transformation. The first transformation, based on an estimated noise covariance matrix, decorrelates and rescales the noise in the data. This step results in a set of noise-whitened data in which the noise covariance matrix is the identity matrix. The second step is a standard PC transformation of the noise-whitened data. After the MNF transform, the data space can be divided into two parts: one part associated with large eigenvalues and coherent eigenimages, and a complementary part with near-unity eigenvalues and noise-dominated images. The coherent eigenimages are noise segregated and dimension reduced images. It is recommended that the LS unmixing should be applied to the eigenimages only.

4 EXPERIMENTS

4.1 Test Image

The test image (figure 1), downloaded from the web at URL: http://dynamo.ecn.purdue/~biehl/MultiSpec/, is a portion of the AVIRIS hyperspectral data taken over an agricultural area of NW Indiana in the early growing season of 1992. The image has the size of 85 rows by 65 columns and 220 bands. Its corresponding ground truth map is shown in figure 2. The crop canopies had only 5% cover, the rest being soil covered with the residue of previous year crop. The label 'notill' is an indication of a large amount of residue and 'min' indicates a small amount of residue.

Figure 1: The test image.

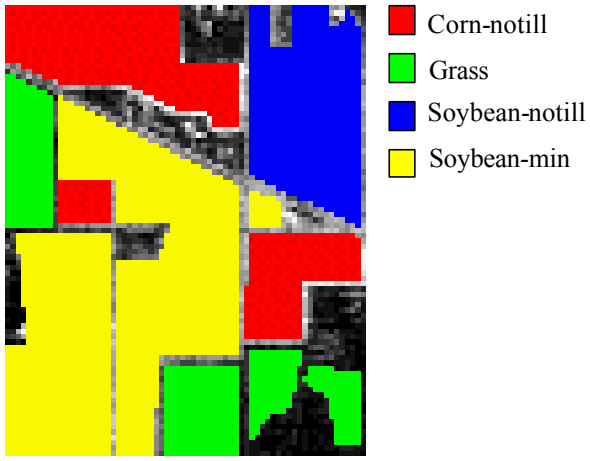

Figure 2: The ground truth map.

For the experiments, the endmember spectra of the ground objects were obtained by taking the average spectrum of the pixels within the area covered by each class. The ground truth data are also used as test samples to estimate the accuracy of the classification results.

4.2 The MNF Transformation

To segregate the image noise and to extract the most signal from the original bands, the MNF transformation was applied to the test image. For the transformation, the noise statistics were estimated from the data. A shift-difference is performed on a selected homogeneous area of the image by differencing adjacent pixels to the right and above each pixel and averaging the results to estimate the noise of the pixel. After the transformation, the first 20 eigenimages were selected as a new set of data of 20 MNF bands. The cutoff number is determined by checking the MNF eigenvalue plot shown in figure 3.

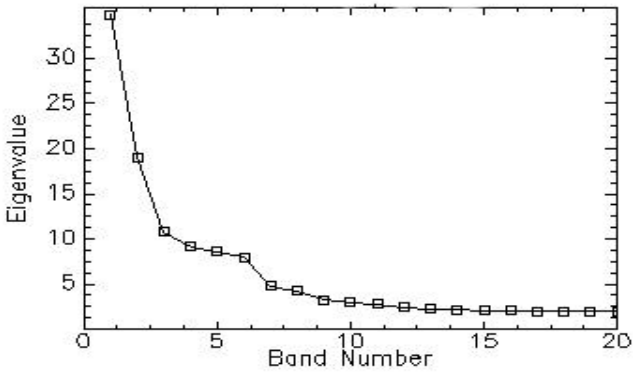

Figure 3: The MNF eigenvalue plot.

4.3 Spectral Unmixing and Classification

The process of spectral unmixing was firstly proceeded with the original image. Figure 4 and figure 5 show the class fraction images and the class map resulted from the LS unmixing and the MF unmixing respectively. Although the class fraction images represent the consequences of subpixel classification, they do not show directly the distribution of classified areas. However, a class map, which is a pixel-based representation of classification, can be generated by choosing the class with the largest pixel value in the fraction images for output.

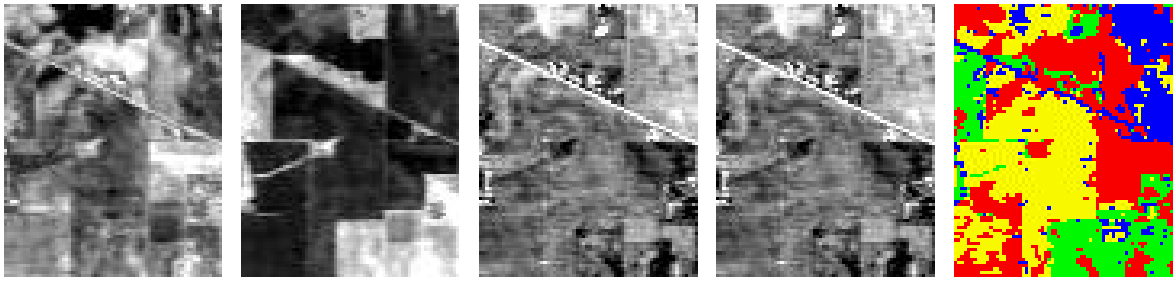

Figure 4: The class fraction images and class map resulted from the LS unmixing performed on the original image.

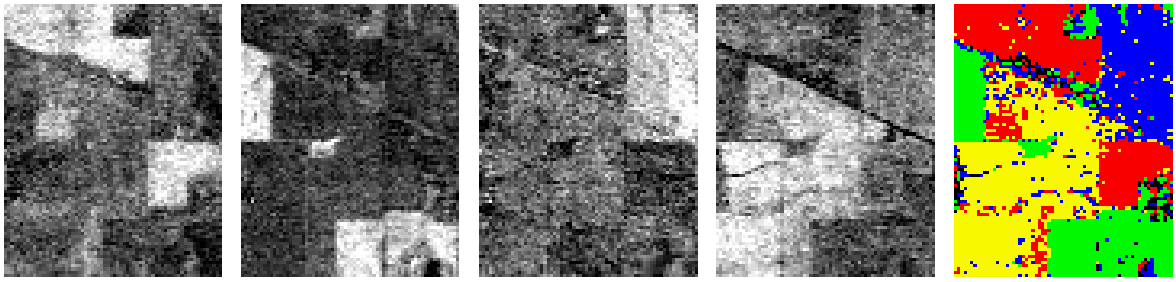

Figure 5: The class fraction images and class map resulted from the MF unmixing performed on the original image.

The second experiment for unmixing was carried out with the 20 MNF bands extracted from the original image. Figure 6 and figure 7 show the class fraction images and class map resulted from the LS unmixing and the MF unmixing respectively.

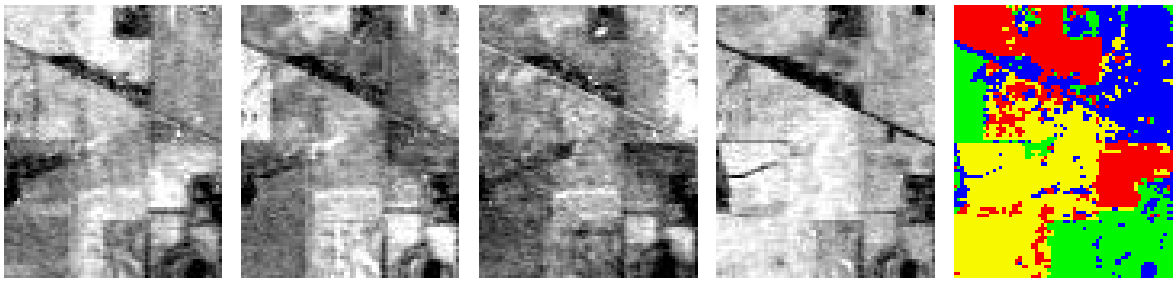

Figure 6: The class fraction images and class map resulted from the LS unmixing performed on the 20 MNF bands.

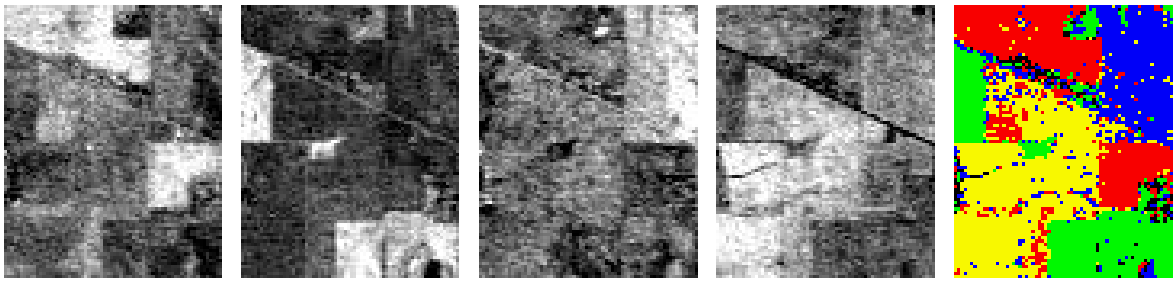

Figure 7: The class fraction images and class map resulted from the MF unmixing performed on the 20 MNF bands.

No evaluation methods are known for sub-pixel classification. The class map represents the results of pixel-based classification. In this paper, therefore, traditional pixel-based accuracy assessment is adopted alternatively to evaluate the performance of sub-pixel classification. Table 1 shows the error matrices resulted from the 4 classification methods. It can be seen that misclassification happens mostly in-between the classes of Corn-notill and Soybean-min, and the LS

unmixing with the original image has the worst performance. Table 2 shows the statistical data of the accuracy assessment.

Table 1: The error matrices resulted from the 4 difference classification methods.

Method	LSU				MFU				LSU_MNF				MFU_MNF			
Ref.	Corn	Grass	Soy1	Soy2	Corn	Grass	Soy1	Soy2	Corn	Grass	Soy1	Soy2	Corn	Grass	Soy1	Soy2
Corn	651	0	49	298	943	0	13	42	872	18	28	80	933	0	12	53
Grass	51	547	67	37	0	699	3	0	0	680	20	2	0	698	4	0
Soy1	227	0	441	59	11	1	684	31	12	3	654	58	10	2	664	51
Soy2	492	16	59	1338	147	10	133	1615	201	4	163	1537	162	8	147	1588

Table 2: The estimates of overall accuracy (OA) and Kappa coefficient ($\hat{\kappa}$) for the classification methods.

		LSU	MFU	LSU_MNF	MFU_MNF
OA (%)		68.7	91.0	86.4	89.6
$\hat{\kappa}$ (%)		63.7	89.3	83.9	87.8
Com-mission (%)	Corn	77.1	15.8	21.3	17.2
	Grass	2.3	1.6	3.6	1.4
	Soy1	24.1	20.5	29.0	22.4
	Soy2	20.7	3.8	7.3	5.5
Omis-sion (%)	Corn	34.8	5.5	12.6	6.5
	Grass	22.1	0.4	3.1	0.6
	Soy1	39.3	5.9	10.0	8.7
	Soy2	29.8	15.2	19.3	16.6

When the original images is used, the MF unmixing outrivals the LS unmixing in classification accuracy. The LS unmixing gets low classification accuracy mainly due to the large commission error of the Corn-notill class. The MNF transform is proved to be a great help to the LS unmixing. The use of the MNF transformed images improves the classification accuracy of the LS unmixing for about 20%.

5 CONCLUSIONS

Sub-pixel classification of hyperspectral images using spectral unmixing techniques is promising. The MF unmixing method proved itself to be an effective technique in classifying a hyperspectral image by showing a 90% classification accuracy. Although the LS unmixing technique did not show promising results when it was applied to the original bands of the test image, its performance can be promoted as long as image noise is segregated. Applying the LS unmixing to the MNF transformed images can improve the classification accuracy for about 20%.

Although conventional pixel-based accuracy assessment is in a sense still available for the evaluation of sub-pixel classification, it does not take full use of the information content of the data resulted from the sub-pixel classification. However, an appropriate accuracy assessment for sub-pixel classification is needed in the future. In fact, Foody (1999) pointed out that the use of sub-pixel classification does not fully solve the mixed-pixel problem. The spectral mixture problem should be considered in the whole classification process, i.e., in the training, classification, and evaluation stages, so that a continuum of classification fuzziness is defined. In view of this proposition, techniques to solve spectral unmixing problem should accommodate spectral mixture into the whole classification process, through the stages of endmember selection, unmixing, and accuracy assessment.

ACKNOWLEDGMENTS

This research project was sponsored by the National Science Council of Republic of China under the grants of NSC88-2211-E006-051.

REFERNENCES

Boardman, J. W. (1994). Geometric Mixture Analysis of Imaging Spectrometry Data. International Geoscience and Remote Sensing Symposium (IGARSS '94), pp. 2369-2371.

Bowles, J., Palmadesso, P., Antoniades, J., Baumback, M., and Rickard, L. J. (1995). Uses of Filter Vectors in Hyperspectral Data Analysis. SPIE, pp. 148-157.

Foody, G. M. (1999). The Continuum of Classification Fuzziness in Thematic Mapping, Photogrammetric Engineering & Remote Sensing, 65(4), pp. 443-451.

Goetz, A. F. H., Vane, G., Solomon, J. E., and Rock, B. N. (1985). Imaging spectrometry for Earth remote sensing, Science, 228, pp. 1147-1153.

Green, A. A., Berman, M., Switzer, P., and Craig, M. D. (1988). A Transformation for Ordering Multispectral Data in Terms of Image Quality with Implications for Noise Removal, IEEE Transactions on Geoscience and Remote Sensing, 26(1), pp. 65-74.

Horwitz, H. M., Nalepka, R. F., Hyde, P. D., and Morgenstern, J. P. (1971). Estimating the proportions of objects within a single resolution element of a multispectral scanner. The 7th International Symposium on Remote Sensing of Environment, Ann Arbor, Michigan, pp. 1307-1320.

Pesses, M. E. (1999). A Least-Squares-Filter Vector Hybrid Approach to Hyperspectral Subpixel Demixing, IEEE Transactions on Geoscience and Remote Sensing, 37(2), pp. 846-849.

Shimabukuro, Y. E., and Smith, J. A. (1991). The least-squares mixing models to generate fraction images derived from remote sensing multispectral data, IEEE Transactions on Geoscience and Remote Sensing, 29(1), pp. 16-20.

Singh, A., and Harrison, A. (1985). Standardized Principal Components, International Journal of Remote Sensing, 6, pp. 883-896.